



# MiR-26a functions as a tumor suppressor in ambient particulate matter-bound metal-triggered lung cancer cell metastasis by targeting LIN28B–IL6–STAT3 axis

Yan-Yang Lu<sup>1,3,4</sup> · Yi Lin<sup>1,3</sup> · Dong-Xiao Ding<sup>1,3,4</sup> · Shu Su<sup>2</sup> · Qiao-Qiao Chi<sup>3</sup> · You-Chi Zhang<sup>3</sup> · Jian Sun<sup>3</sup> · Xu Zhang<sup>1,3,4</sup> · Hui-Min Zhu<sup>1,3</sup> · Qian-Sheng Huang<sup>1,3</sup> · Yu-Lang Chi<sup>1,3</sup> · Guo-Zhu Ye<sup>1,3</sup> · Shu Tao<sup>2</sup> · Si-Jun Dong<sup>1,3</sup>

Received: 20 July 2017 / Accepted: 5 December 2017 / Published online: 8 December 2017  
© Springer-Verlag GmbH Germany, part of Springer Nature 2017

## Abstract

Exposure to ambient particulate matter (PM) has been linked to the increasing incidence and mortality of lung cancer, but the principal toxic components and molecular mechanism remain to be further elucidated. In this study, human lung adenocarcinoma A549 cells were treated with serial concentrations of water-extracted PM<sub>10</sub> (WE-PM<sub>10</sub>) collected from Beijing, China. Our results showed that exposure to 25 and 50 µg/ml of WE-PM<sub>10</sub> for 48 h significantly suppressed miR-26a to upregulate lin-28 homolog B (LIN28B), and in turn activated interleukin 6 (IL6) and signal transducer and activator of transcription 3 (STAT3) in A549 cells, subsequently contributing to enhanced epithelial–mesenchymal transition and accelerated migration and invasion. In vivo pulmonary colonization assay further indicated that WE-PM<sub>10</sub> enhanced the metastatic ability of A549 cells. In addition, luciferase reporter assay demonstrated that 3' untranslated region of *LIN28B* was a direct target of miR-26a. Last but not the least, the key toxic contribution of metals in WE-PM<sub>10</sub> was confirmed by the finding that removal of metals through chelation significantly rescued WE-PM<sub>10</sub>-mediated inflammatory, carcinogenic and metastatic responses. Taken together, miR-26a could act as the tumor suppressor in PM<sub>10</sub>-related lung cancer, and PM<sub>10</sub>-bound metals promoted lung cancer cell metastasis through downregulation of miR-26a that directly mediated LIN28B expression.

**Keywords** Water-extracted PM<sub>10</sub> (WE-PM<sub>10</sub>) · Metals · MiR-26a · Migration · Invasion · Inflammation

Yan-Yang Lu and Yi Lin contributed equally to this work.

**Electronic supplementary material** The online version of this article (<https://doi.org/10.1007/s00204-017-2141-4>) contains supplementary material, which is available to authorized users.

✉ Yi Lin  
ylin@iue.ac.cn

✉ Si-Jun Dong  
sjdong@iue.ac.cn

<sup>1</sup> Center for Excellence in Regional Atmospheric Environment, Institute of Urban Environment, Chinese Academy of Sciences, Xiamen 361021, China

<sup>2</sup> Laboratory for Earth Surface Processes, College of Urban and Environmental Sciences, Peking University, Beijing 100871, China

<sup>3</sup> Key Lab of Urban Environment and Health, Institute of Urban Environment, Chinese Academy of Sciences, Xiamen 361021, China

<sup>4</sup> College of Resources and Environment, University of Chinese Academy of Sciences, Beijing 100049, China

## Introduction

Ambient particulate matter (PM) can penetrate deeply into the respiratory system, which has been linked to the occurrence and exacerbation of respiratory diseases in humans, such as asthma, chronic obstructive pulmonary disease and lung cancer (Guan et al. 2016). For example, a meta-analysis using large amounts of data from 17 cohort studies in nine European countries showed an association between long-term exposure to PM and the incidence of lung cancer, particularly lung adenocarcinoma. Furthermore, this study suggested that exposure to PM increased the risk of lung cancer even at concentrations below annual limit values of the European Union air quality standards for PM<sub>10</sub> (40 µg/m<sup>3</sup>) and PM<sub>2.5</sub> (25 µg/m<sup>3</sup>) (Raaschou-Nielsen et al. 2013). In China, ambient PM levels remain substantially higher than those in developed countries (Xu et al. 2016). Cohort studies with data of the National Cancer Registration of China from 1990 to 2009 showed that each 10 µg/m<sup>3</sup> increase of PM<sub>2.5</sub> was associated with relative risks of lung cancer incidence

in both males (1.055, 95% CI: 1.038–1.072) and females (1.149, CI: 1.120–1.178) (Guo et al. 2016) and, moreover, PM<sub>2.5</sub> was positively associated with lung cancer mortality in China (Guo et al. 2017). In addition to PM<sub>2.5</sub>, a cohort with data collected from 39,054 Chinese participants during 1998–2009 also clearly showed that each 10 µg/m<sup>3</sup> increase in PM<sub>10</sub> was associated with a significant 3.4–6.0% increase in the risk of lung cancer mortality (Chen et al. 2016). The International Agency for Research on Cancer (IARC) has classified PM in outdoor air as a Group I carcinogen and confirmed that exposure to PM increased the risk of lung cancer (Hamra et al. 2014).

MicroRNAs (MiRNAs) are considered as an important molecular mechanism through which PM impairs cellular homeostasis and function, leading to the development of lung inflammation and lung cancer (Jardim et al. 2009; Wei et al. 2015). Jardim et al. first reported that diesel exhaust particles (DEPs) altered miRNA expression profiles in human airway epithelial cells, and subsequently changed cellular processes and induced diseases by regulating genes in inflammatory and tumorigenesis-associated pathways (Jardim et al. 2009). MiR-802/Rnd3 pathway was also found to play an important role in PM-triggered carcinogenesis and metastasis in pulmonary cells (Li et al. 2016). In human populations, downregulation of miR-144 was reported to be critical for air pollution-related lung cancer in Xuanwei, China, where PM was generated by the combustion of bituminous coal (Pan et al. 2015); but notably, this study indicated that treatment of human bronchial epithelial cells with some polycyclic aromatic hydrocarbons (PAHs) adsorbed in PM, such as BaP, BPDE, and BzP, did not result in the downregulation of miR-144, implying that other components in PM may contribute to the downregulation of this miRNA. Indeed, PM-associated toxicity depends to a large extent on its components; however, it is still unclear which the most harmful component of PM is. Besides PAHs, metallic elements, including PM<sub>2.5</sub> Cu, PM<sub>10</sub> Zn, PM<sub>10</sub> S, PM<sub>10</sub> Ni and PM<sub>10</sub> K, were reported to be associated with elevated hazard ratios for lung cancer in participants who did not change residence during 13.1 years of follow-up in a meta-analysis using data of 14 cohort studies in eight European countries (Raaschou-Nielsen et al. 2016). Weekly exposure to Cr- and Ni-containing welding PM was also found to initiate inflammation and increase the number of malignant lung lesions in male mice (Zeidler-Erdely et al. 2013). IARC has designated As, Ni, Cr compounds as Group I carcinogens and Pb compound as a Group II A carcinogen (IARC 2012). Whether metals present in ambient PM could be responsible for lung carcinogenesis and metastasis needs to be further elucidated.

In the present study, we treated human lung adenocarcinoma A549 cells with water-extracted PM<sub>10</sub> (WE-PM<sub>10</sub>) and confirmed that metals were key contributors to the inflammatory and carcinogenic effects of Beijing PM<sub>10</sub>. Furthermore,

we provided a novel mechanism that PM<sub>10</sub>-bound metals downregulated miR-26a to activate Lin-28 homolog B–interleukin 6–signal transducer and activator of transcription 3 (LIN28B–IL6–STAT3) axis, and ultimately promoted tumor cell metastasis.

## Materials and methods

### PM<sub>10</sub> collection and sample solution preparation

PM<sub>10</sub> samples were kindly gifted by Dr. Shu Tao (Peking University). As in a previous study (Wang et al. 2013), PM<sub>10</sub> samples were collected in Peking University campus (N39°59′26″, E116°18′12″) using a median volume active sampler in November 2014. Glass fiber filters were used as a sampling medium. To extract aqueous fraction, PM<sub>10</sub> filters were sonicated in ultrapure water for 3 × 30 min. The extracts were filtered, lyophilized, and re-suspended in sterile water prior to use (WE-PM<sub>10</sub>). To remove metals from WE-PM<sub>10</sub>, the WE-PM<sub>10</sub> solution was processed through a miniature column of Chelex 100 resin (Bio-Rad, #143–2832, Hercules CA, USA) (Chel-WE-PM<sub>10</sub>) as reported (Pardo et al. 2015).

### Quantitative analysis of metal elements

WE-PM<sub>10</sub> and Chel-WE-PM<sub>10</sub> were digested with a mixture of HNO<sub>3</sub> and HCl (Mars 5; CEM Incorporation, NC, USA) and the metallic elements were determined using inductively coupled plasma mass spectrometry (ICP-MS; Agilent 7500cx, Agilent Technologies Incorporation, CA, USA) and inductively coupled plasma optical emission spectrometer (ICP-OES; Optima 7000 DV, PerkinElmer, USA) (Rodriguez-Cotto et al. 2014).

### Cell culture and treatment

The human lung adenocarcinoma A549 cells were purchased from the cell bank of Type Culture Collection of Chinese Academy of Sciences (Shanghai, China). Cells were maintained in DME/F12 medium (HyClone, Logan, UT) supplemented with 10% FBS and were exposed to serial concentrations of WE-PM<sub>10</sub> (0, 5, 25, and 50 µg/ml) or Chel-WE-PM<sub>10</sub> (metals were removed from 50 µg/ml of WE-PM<sub>10</sub>) for 48 h. For miR-26a overexpression and inhibition, A549 cells were transfected with 50 nM of miR-26a mimic or 300 nM of miR-26a inhibitor (RiboBio, Guangzhou, China) for 48 h, respectively (Supplementary material: Fig. S1). For LIN28B knockdown, A549 cells were transfected with LIN28B siRNA (36 nM, Santa Cruz) for 48 h following the manufacturer's instructions (Supplementary material: Fig. S2).

## In vivo tumor metastasis assay

Male BALB/c nude mice (16–20 g) were purchased from the SLAC Laboratory Animal Co. Ltd (Shanghai, China). After appropriate pretreatment processes,  $8 \times 10^4$  cells per mouse were injected into the tail vein of nude mice. The mice were killed 4 weeks after injection, and the lung and liver metastases were determined using H&E staining.

## Cell migration and invasion assays

24-well transwell plates with polycarbonate membrane inserts (pore size, 8.0  $\mu\text{m}$ ; Corning, ME, USA) were used to measure migration and invasion potential of A549 cells. For migration assay, cells were added into the upper chamber at a density of approximately  $2 \times 10^4$  cells/well. Complete medium was placed into the bottom chamber. After a 6-h incubation, the cells that migrated to the lower surface of the membrane were fixed with methanol, air-dried, and stained with 0.1% crystal violet. To study invasion, the upper surface of the filter was coated with 20–30  $\mu\text{g}$  of Matrigel (BD Biosciences, MA, USA) and  $3 \times 10^4$  cells/well were added into the upper chamber. After a 24-h incubation, the invasive cells were fixed and stained as described above. Cell migration and invasion ability were determined by calculating the cell number on the lower surface of the filter in five random microscopic fields chosen from the top, bottom, left, right, and center position of each filter.

## Determination of IL6 secretion

The levels of IL6 in cell culture supernatants were measured by enzyme-linked immunosorbent assay (ELISA; eBioscience, CA, USA). The concentrations of IL6 were normalized to protein content.

## Luciferase reporter assay

The 3' untranslated region (3' UTR) of *LIN28B* harboring a DNA fragment with the wild-type or mutated miR-26a binding site was amplified from human cDNA using primers shown in Supplementary material: Table S1, and then sub-cloned into the pmirGLO dual-luciferase miRNA target expression vector (Promega, WI, USA) named p*LIN28B*-WT-luc and p*LIN28B*-MT-luc, respectively. For the luciferase assay, A549 cells were cotransfected with indicated 3' UTR luciferase reporter vectors and miR-26a mimic or miR-26a inhibitor for 48 h. Luciferase activity was measured using a Dual-Luciferase Reporter Gene Assay System (Promega).

## RNA extraction and real-time PCR

Total RNA was extracted using TRIzol reagent (Thermo Scientific, MA, USA). Real-time PCR was then performed with SYBR® Premix Ex Taq™ II Kit (Takara, Dalian, China) on a LightCycler®480 Instrument II (Roche, Basle, Switzerland). The levels of miRNA and mRNA were normalized to U6 and  $\beta$ -actin, respectively. The primer sequences are described in Supplementary material: Tables S2 and S3.

## Protein extraction and western blot analysis

Protein was extracted with RIPA buffer (Thermo Scientific, IL, USA) and the concentrations were measured using BCA protein assay kit (Thermo Scientific). Equal amounts of protein were subjected to gel electrophoresis and immunoblotted with antibodies against LIN28B (Cell Signaling Technology, MA, USA, #11965, 1:1500), STAT3 (Cell Signaling Technology, #12640, 1:1000), Tyr705-phosphorylated STAT3 (Cell Signaling Technology, #9145, 1:1000), interleukin-6 (Abcam, Cambridge, UK, #ab6672, 1:2000), E-cadherin (Abcam, #ab1416, 1:2000), Vimentin (Abcam, #ab45939, 1:1000) or  $\beta$ -actin (Cell Signaling Technology, #4970, 1:2000).

## Statistical analysis

Data were expressed as mean  $\pm$  SEM. All statistical analyses were conducted with SPSS software v.17.0 (SPSS Inc., Chicago, IL, USA). Multiple-group comparison was analyzed using one-way ANOVA followed by Bonferroni's post hoc test and two-group comparison was determined by unpaired Student's *t* test. Values of  $p < 0.05$  or  $p < 0.01$  were considered statistically significant.

## Results

### WE-PM<sub>10</sub> induced inflammation and promoted invasion and metastasis in A549 cells

As shown in Fig. 1a, 50  $\mu\text{g}/\text{ml}$  WE-PM<sub>10</sub>-exposed A549 cells secreted significantly higher levels of inflammatory cytokine IL6 compared with controls. No difference was detected in the protein levels of proliferating cell nuclear antigen (PCNA, a marker of cell proliferation) between WE-PM<sub>10</sub>-exposed and control cells (Supplementary material: Fig. S3), while exposure to WE-PM<sub>10</sub> resulted in high expression of the epithelial marker E-cadherin (CDH1) and low expression of the mesenchymal marker Vimentin (VIM) (Fig. 1b), suggesting that WE-PM<sub>10</sub> induced EMT-like changes in A549 cells. Results of Boyden chamber assays showed that the number of migratory and invasive

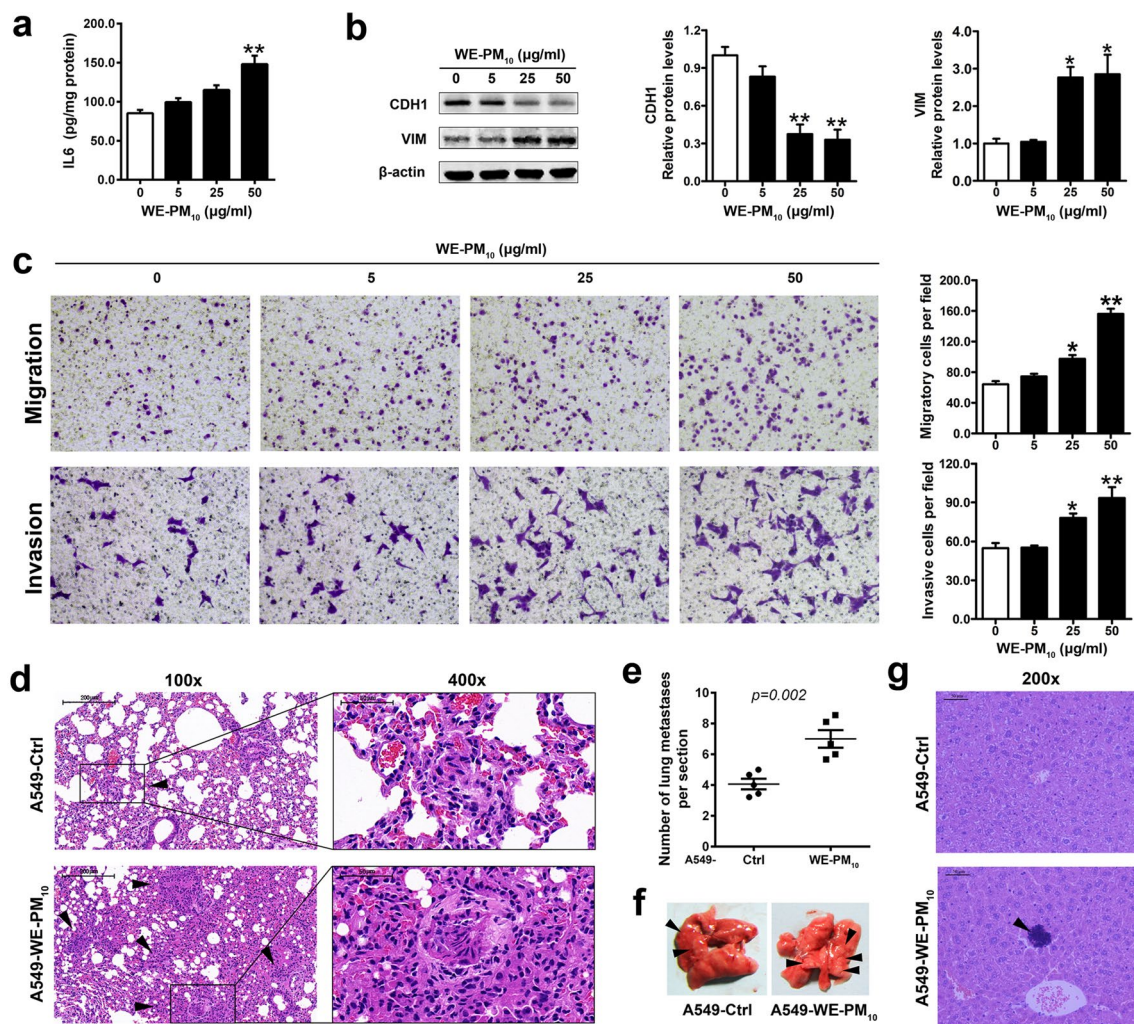


**Fig. 1** WE-PM<sub>10</sub> promoted metastasis in A549 cells. **a** Secretion of IL6. **b** Protein expressions of CDH1 and VIM. **c** Representative photomicrographs ( $\times 100$ ) and average cell number by transwell assays. **d** Representative images of lung metastases ( $\times 100$  and  $\times 400$ ). Arrowheads show microscopic nodules. **e** Average number of lung metastases. **f** Representative photographs of lung tissues. Arrowheads show nodules. **g** Representative liver sections ( $\times 200$ ). The arrow-

head shows the microscopic nodule. For **a–c**, A549 cells were treated with serial concentrations of WE-PM<sub>10</sub> (0, 5, 25, and 50  $\mu\text{g/ml}$ ) for 48 h and data were collected from three independent experiments; and for **d–g**, the nude mice were intravenously injected through tail vein with A549 cells pretreated with 0 (A549-Ctrl) or 50  $\mu\text{g/ml}$  WE-PM<sub>10</sub> (A549-WE-PM<sub>10</sub>) for 48 h and  $n=5$  mice/group. Data are mean  $\pm$  SEM. \* $p < 0.05$ , \*\* $p < 0.01$  vs. controls

cells increased after a 48-h exposure to 25 or 50  $\mu\text{g/ml}$  of WE-PM<sub>10</sub> (Fig. 1c). To further determine the effects of WE-PM<sub>10</sub> on in vivo tumor metastatic potential, nude mice were injected through the tail vein with control (A549-Ctrl) and 50  $\mu\text{g/ml}$  of WE-PM<sub>10</sub>-treated A549 (A549-WE-PM<sub>10</sub>) cells, respectively. Figure 1d–f shows that the number and area of lung metastatic nodules generated by A549-WE-PM<sub>10</sub> cells significantly increased compared with those by A549-Ctrl cells. Moreover, liver metastatic nodules were observed in mice injected with A549-WE-PM<sub>10</sub> cells, and the incidence was 40% (Fig. 1g). In summary, A549 cells underwent inflammation and EMT in response to WE-PM<sub>10</sub>, which was accompanied by an increase in metastatic capacity.

### WE-PM<sub>10</sub> decreased miR-26a and increased LIN28B–IL6–pSTAT3 in A549 cells

MiR-26 exerts a tumor suppressor-like activity in several cancers. As shown in Table 1, treatment of A549 cells with 25 and 50  $\mu\text{g/ml}$  of WE-PM<sub>10</sub> resulted in downregulation of miR-26a, while no distinct difference was observed in miR-26b among groups. Both the mRNA and protein levels of LIN28B were significantly increased in the cells exposed to 50  $\mu\text{g/ml}$  of WE-PM<sub>10</sub> compared with the control (Fig. 2a, c, d). 25  $\mu\text{g/ml}$  of WE-PM<sub>10</sub> also elevated the protein levels of LIN28B in A549 cells. Levels of IL6 mRNA and protein were significantly increased in A549 cells after exposure to 25 and 50  $\mu\text{g/ml}$  of WE-PM<sub>10</sub>

**Table 1** Expression of miR-26a and miR-26b in A549 cells

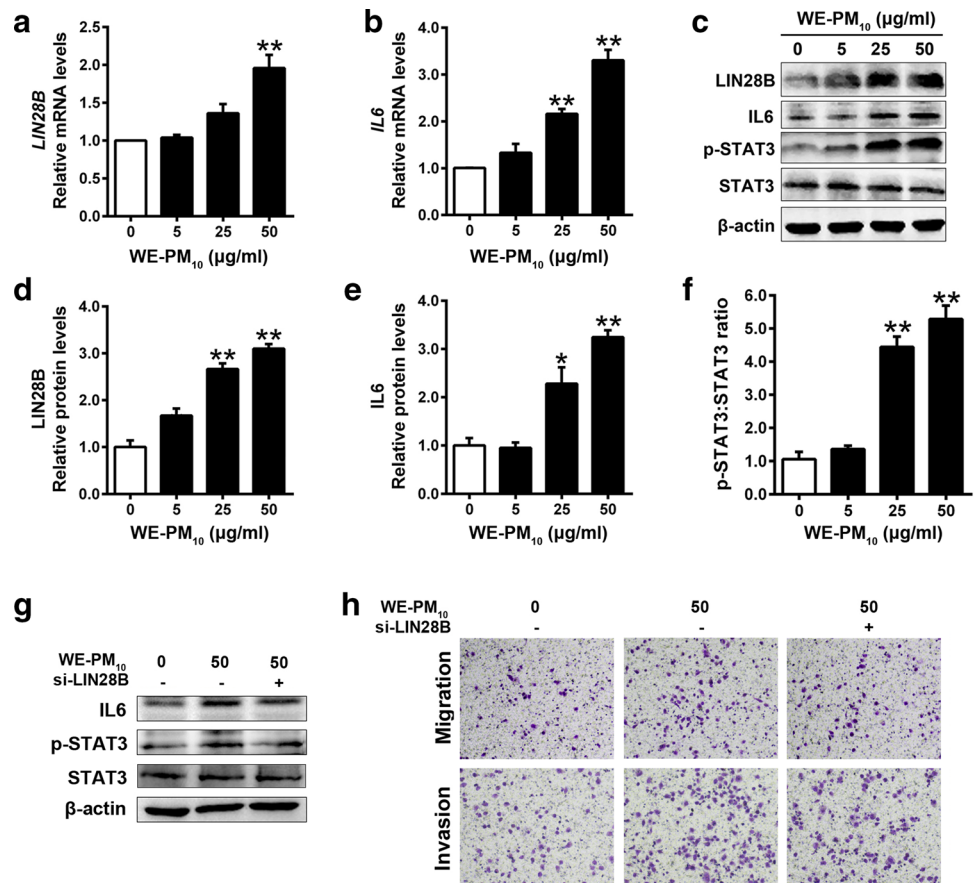
WE-PM <sub>10</sub> (μg/ml)	miR-26a	miR-26b
0	1.00 ± 0.01	1.00 ± 0.01
5	0.89 ± 0.06	0.87 ± 0.18
25	0.77 ± 0.07*	0.83 ± 0.14
50	0.62 ± 0.04**	0.81 ± 0.17

The expression levels of miRNA were normalized to U6 and expressed as fold of values in controls. WE-PM<sub>10</sub>: water-extracted PM<sub>10</sub>. All data are mean ± SEM of three independent experiments

\* $p < 0.05$ , \*\* $p < 0.01$  vs. controls

(Fig. 2b, c, e). Increased phosphorylation of STAT3 (p-STAT3), an effector of IL6, was observed in parallel to the changes in IL6 in 25 and 50 μg/ml WE-PM<sub>10</sub>-exposed A549 cells (Fig. 2c, f). In addition, inhibition of LIN28B by siRNA restored increased IL6 and p-STAT3 (Fig. 2g, Supplementary material: Fig. S4) and enhanced migration and invasion (Fig. 2h, Supplementary material: Fig. S4) in response to 50 μg/ml of WE-PM<sub>10</sub> in A549 cells.

**Fig. 2** WE-PM<sub>10</sub> upregulated LIN28B to increase IL6 and p-STAT3 in A549 cells. For **a–f**, A549 cells were treated with serial concentrations of WE-PM<sub>10</sub> for 48 h; and for **g, h**, cells were cotreated with 50 μg/ml WE-PM<sub>10</sub> and LIN28B siRNA for 48 h. Data are mean ± SEM of three independent experiments. \* $p < 0.05$ , \*\* $p < 0.01$  vs. control cells



## MiR-26a regulated motility and invasiveness of A549 cells via LIN28B–IL 6 axis

The impact of miR-26a on lung tumor cell metastasis was assessed by examining whether the altered expression of miR-26a affected their motility and invasiveness in A549 cells. Figure 3a shows that overexpression of miR-26a significantly reduced the number of migratory and invasive cells compared with the negative control, while endogenous inhibition of miR-26a led to a clear increase in migration and invasion of A549 cells (Fig. 3b). Moreover, Fig. 4a–c shows that both the mRNA and protein levels of LIN28B and IL6 were significantly decreased after transfecting A549 cells with miR-26a mimic. In contrast, additional treatment of miR-26a inhibitor significantly increased the expression of both LIN28B and IL6 (Fig. 4d–f). The crosstalk among miR-26a, LIN28B and IL6 was further determined. Figure 4g, h shows that silencing LIN28B decreased expressions of both IL6 and p-STAT3 (Fig. 4g), but did not affect the expression of miR-26a in A549 cells (Fig. 4h). In addition, A549 cells transfected with miR-26a inhibitor failed to increase protein expressions of IL6 and p-STAT3, migration and invasion when LIN28B was knocked down (Figs. 3c, 4 g).

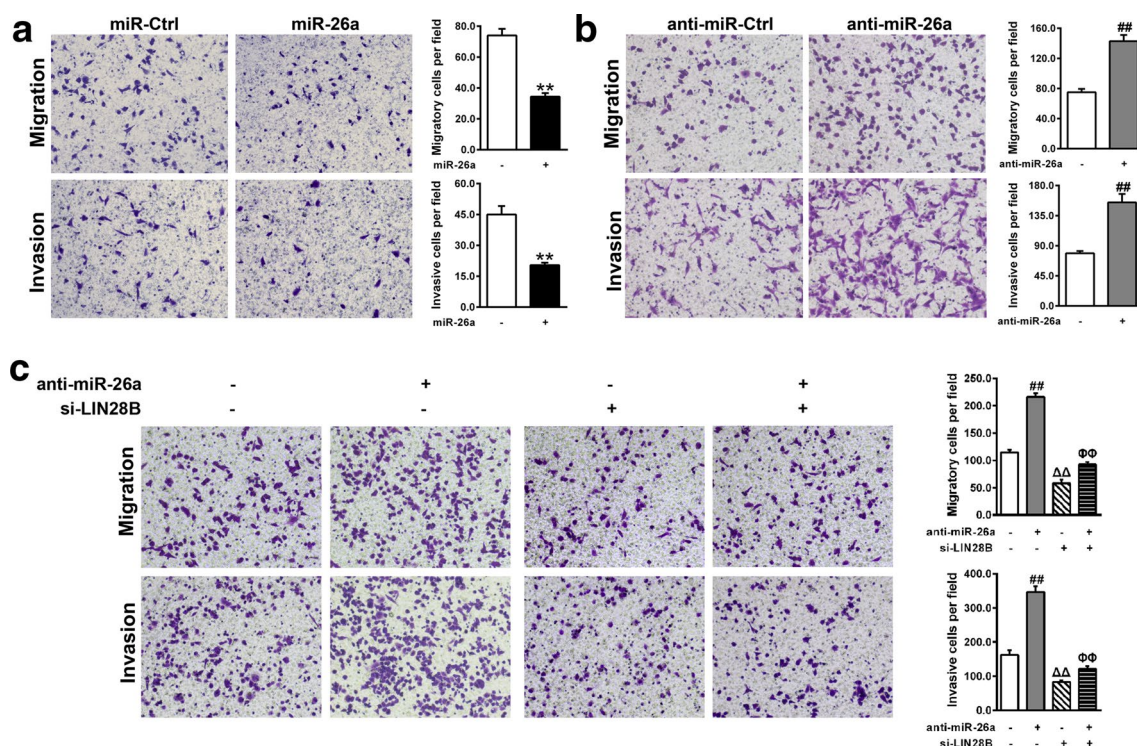


**Fig. 3** MiR-26a suppressed migration and invasion of A549 cells. Representative photomicrographs (100 $\times$ ) and average cell number by transwell migration and invasion assays. For **a** and **b**, A549 cells were transfected with miR-26a mimic or miR-26a inhibitor for 48 h, and for **c**, A549 cells were cotransfected with miR-26a inhibitor and LIN28B siRNA for 48 h. Data are mean  $\pm$  SEM of three independent experiments. \*\* $p$  < 0.01 vs. cells transfected with mimic control;

## $p$  < 0.01 vs. cells transfected with inhibitor control;  $\Delta\Delta p$  < 0.01 LIN28B siRNA-treated cells cotransfected with inhibitor control vs. siRNA control-treated cells cotransfected with inhibitor control;  $\Phi\Phi p$  < 0.01 miR-26a inhibitor-treated cells cotransfected with LIN28B siRNA vs. miR-26a inhibitor-treated cells cotransfected with control siRNA

### LIN28B was a direct target of miR-26a

As shown in Fig. 5a, miR-26a has a binding site in the *LIN28B* 3' UTR. Figure 5b shows that overexpression of miR-26a reduced the luciferase activity of a reporter gene fused truncated *LIN28B*-3' UTR sequence harboring a DNA fragment with the predicted miR-26a binding site, and mutation in this binding site abolished the reduction of luciferase activity in A549 cells. Conversely, miR-26a inhibitor increased the luciferase activity and this inducible effect was abolished when the predicted binding site was mutated (Fig. 5c). Therefore, miR-26a regulated *LIN28B* by directly targeting its 3' UTR.

### Overexpression of miR-26a abrogated WE-PM<sub>10</sub>-induced lung cancer cell metastasis

To ascertain that WE-PM<sub>10</sub>-induced upregulation of LIN28B and IL6 in A549 cells was attributed to the downregulation of miR-26a, A549 cells were treated

with 50  $\mu$ g/ml of WE-PM<sub>10</sub> and transfected with miR-26a mimic. Figure 6a–c shows that restoration of miR-26a in WE-PM<sub>10</sub>-exposed A549 cells significantly abrogated the higher mRNA and protein expressions of LIN28B and IL6. Likewise, restoration of miR-26a significantly suppressed the enhancement of both migration and invasion in 50  $\mu$ g/ml WE-PM<sub>10</sub>-exposed A549 cells (Fig. 6d). To further observe the influence of miR-26a on WE-PM<sub>10</sub>-associated tumor metastasis in vivo, we employed nude mice that were injected with A549 cells which were transfected with mimic control or miR-26a mimic prior to 50  $\mu$ g/ml of WE-PM<sub>10</sub> treatment (A549-miR-Ctrl-WE-PM<sub>10</sub>, A549-miR-26a-WE-PM<sub>10</sub>). Figure 6e shows that the size and number of lung metastatic nodules in nude mice injected with A549-miR-26a-WE-PM<sub>10</sub> were significantly decreased compared with those in A549-miR-Ctrl-WE-PM<sub>10</sub> group. Taken together, miR-26a suppressed WE-PM<sub>10</sub>-enhanced metastatic potential of human lung cancer cells, which might occur via downregulating LIN28B and IL6.

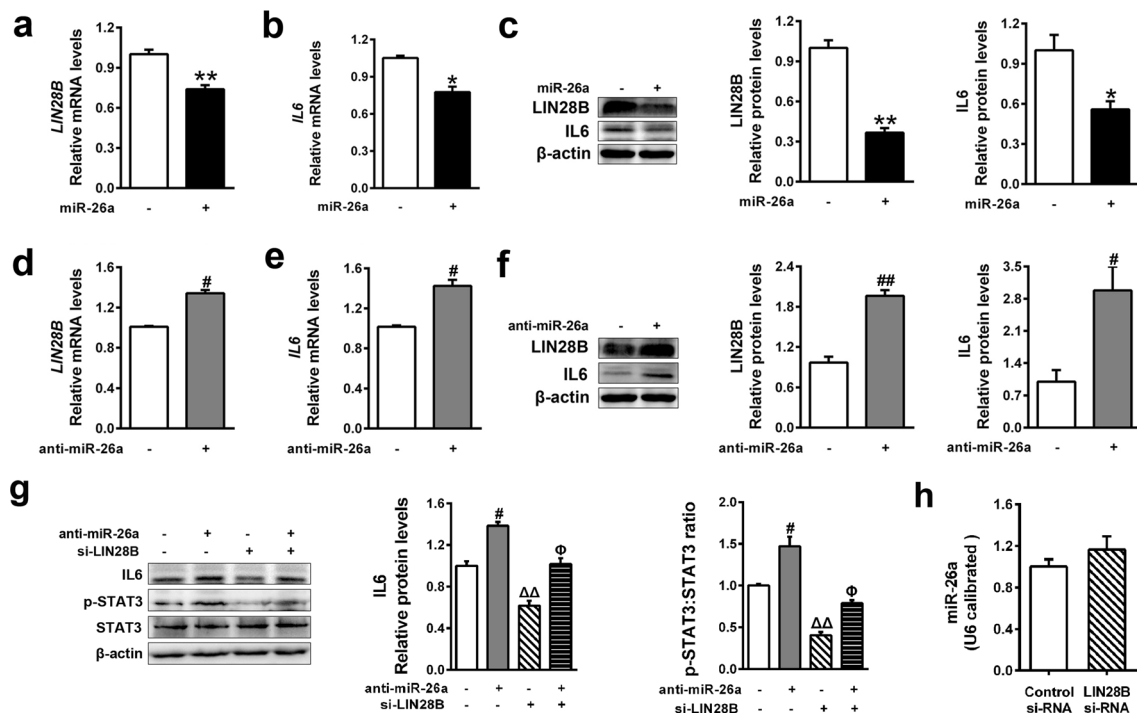


**Fig. 4** LIN28B and IL6 were targets of miR-26a. **a, d** mRNA expression of LIN28B. **b** and **e** mRNA expression of IL6. **c, f** Protein expressions of LIN28B and IL6. **g** Protein expressions of IL6 and p-STAT3. **h** Expression of miR-26a. For **a–c**, A549 cells were transfected with miR-26a mimic for 48 h; for **d–f**, A549 cells were transfected with miR-26a inhibitor for 48 h; for **g**, A549 cells were cotransfected with miR-26a inhibitor and LIN28B siRNA for 48 h; and for **h**, A549 cells were transfected with LIN28B siRNA for 48 h.

Data are mean  $\pm$  SEM of three independent experiments. \* $p$  < 0.05, \*\* $p$  < 0.01 vs. cells transfected with mimic control; # $p$  < 0.05, ## $p$  < 0.01 vs. cells transfected with inhibitor control;  $\Delta p$  < 0.05,  $\Delta\Delta p$  < 0.01 LIN28B siRNA-treated cells cotransfected with inhibitor control vs. siRNA control-treated cells cotransfected with inhibitor control;  $\Phi p$  < 0.05,  $\Phi\Phi p$  < 0.01 miR-26a inhibitor-treated cells cotransfected with LIN28B siRNA vs. miR-26a inhibitor-treated cells cotransfected with control siRNA

## Contributions of metals to lung cancer cell inflammation and metastasis

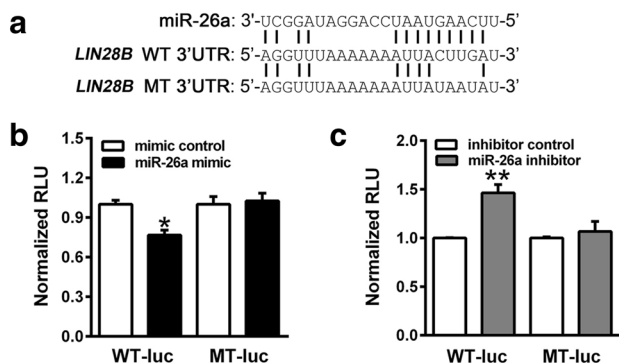


**Fig. 5** LIN28B was a direct target of miR-26a. **a** MiR-26a target regions in the 3' UTR of LIN28B. **b** and **c** Relative luciferase activity in A549 cells transfected with reporter gene containing the 3' UTR of LIN28B in its constructs, together with either miR-26a mimic (**b**), miR-26a inhibitor (**c**) or corresponding controls. WT: a truncated LIN28B-3'UTR with wild-type miR-26a binding site; MT: a truncated LIN28B-3'UTR with mutated miR-26a binding site. Data are mean  $\pm$  SEM of three independent experiments. \* $p$  < 0.05, \*\* $p$  < 0.01 vs. corresponding controls

Metals were removed from WE-PM<sub>10</sub> by chelation on a Chelex column (Chel-WE-PM<sub>10</sub>) and Table 2 shows that approximately 98.57% of metals were successfully removed by this process. Interestingly, exposure to Chel-WE-PM<sub>10</sub> did not alter the expression of miR-26a, as well as LIN28B, IL6 and p-STAT3 (Fig. 7a–d, Supplementary material: Fig. S5). Moreover, removal of metals abrogated WE-PM<sub>10</sub>-induced production and secretion of IL6 in A549 cells (Fig. 7e). Paralleling the inflammation evidence, Chel-WE-PM<sub>10</sub> did not trigger EMT (Fig. 7d, Supplementary material: Fig. S5) and promote migration and invasion in A549 cells (Fig. 7f). In nude mice injected with Chel-WE-PM<sub>10</sub>-treated A549 cells (A549-Chel-WE-PM<sub>10</sub>), the number and size of lung metastatic nodules were comparable with those injected with A549-Ctrl cells but less than those injected with A549-WE-PM<sub>10</sub> cells (Fig. 7g). Therefore, metals should be one of the major contributors to the initiation of inflammatory, carcinogenic and metastatic responses in WE-PM<sub>10</sub>-exposed A549 cells.

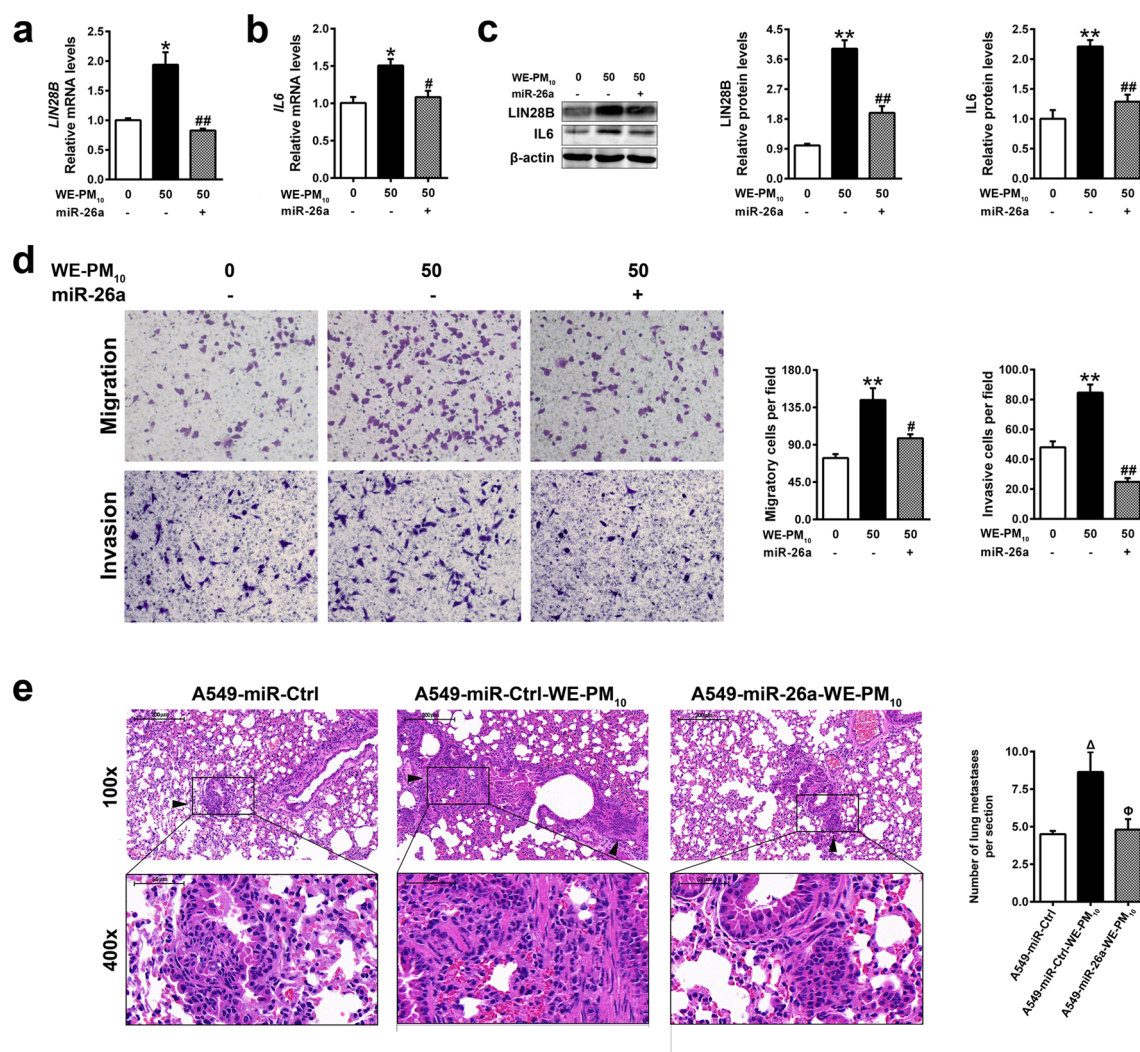


**Fig. 6** Overexpression of miR-26a abrogated WE-PM<sub>10</sub>-induced metastasis of lung cancer cells. **a, b** mRNA expressions of LIN28B and IL6. **c** Protein expressions of LIN28B and IL6. **d** Representative photomicrographs ( $\times 100$ ) and average cell number by transwell assays. **e** Representative images ( $\times 100$  and  $\times 400$ ) and quantification of lung metastases. Arrowheads show microscopic nodules. A549-miR-Ctrl: nude mice were injected with A549 cells transfected with mimic control; A549-miR-Ctrl-WE-PM<sub>10</sub>: nude mice were injected with A549 cells treated with mimic control and 50  $\mu\text{g}/\text{ml}$  WE-PM<sub>10</sub>;

A549-miR-26a-WE-PM<sub>10</sub>: nude mice were injected with A549 cells treated with miR-26a mimic and 50  $\mu\text{g}/\text{ml}$  WE-PM<sub>10</sub>. For **a–d**, A549 cells were transfected with mimic control or miR-26a mimic and exposed to 50  $\mu\text{g}/\text{ml}$  of WE-PM<sub>10</sub>. Data were collected from three independent experiments; and for **(e)**,  $n=5$  mice/group. Data are mean  $\pm$  SEM. \* $p < 0.05$ , \*\* $p < 0.01$  vs. control cells transfected with mimic control; # $p < 0.05$ , ## $p < 0.01$  vs. WE-PM<sub>10</sub>-exposed cells transfected with mimic control;  $\Delta p < 0.05$  vs. mice in A549-miR-Ctrl group;  $\Phi p < 0.05$  vs. mice in A549-miR-Ctrl-WE-PM<sub>10</sub> group

## Discussion

Exposure to PM<sub>10</sub> has been considered as an important risk factor for lung cancer, which is the most frequently diagnosed cancer and the first leading cause of cancer-related deaths in China (Chen et al. 2017b). In this study, we showed that a 48-h exposure to 25 and 50  $\mu\text{g}/\text{ml}$  (approximately equal to 5 and 10  $\mu\text{g}/\text{cm}^2$ ) water-extracted PM<sub>10</sub> collected in Beijing (WE-PM<sub>10</sub>) upregulated LIN28B and IL6 through the inhibition of miR-26a, consequently inducing EMT in human lung adenocarcinoma A549 cells and promoting

tumor cell migration and invasion. Similarly, a recent study indicated that 16  $\mu\text{g}/\text{cm}^2$  of PM<sub>2.5</sub> collected in Beijing promoted EMT, migration and invasion of A549 cells (Deng et al. 2017). Besides in China, 10  $\mu\text{g}/\text{cm}^2$  of PM<sub>10</sub> from urban commercial zone in Mexico has been reported to increase invasiveness and alter expression of EMT markers (E-cadherin and  $\beta$ -catenin) in A549 cells (Morales-Barcenas et al. 2015), and long-term exposure to 100  $\mu\text{g}/\text{ml}$  standard reference material (SRM) of atmospheric particulate matter was found to enhance carcinogenesis and metastasis of A549 cells (Li et al. 2016). Abnormal induction of

**Table 2** Concentrations of metals in WE-PM<sub>10</sub> and Chel-WE-PM<sub>10</sub>

Elements	WE-PM <sub>10</sub> (µg/g)	Chel-WE-PM <sub>10</sub> (µg/g)
Ca	58818.46 ± 1446.41	319.24 ± 66.47
K	17284.23 ± 235.36	144.09 ± 8.43
Na	16263.53 ± 576.82	–
Mg	6355.35 ± 194.03	19.72 ± 4.47
Zn	4284.09 ± 143.75	7.38 ± 2.10
Al	2521.00 ± 150.12	74.22 ± 2.63
Fe	1722.42 ± 19.36	208.01 ± 8.17
B	754.24 ± 28.86	648.23 ± 1.96
Ba	597.77 ± 14.44	1.29 ± 0.03
Mn	529.67 ± 12.82	1.29 ± 0.72
Cu	371.66 ± 27.04	23.33 ± 1.53
Sr	311.26 ± 10.34	0.46 ± 0.10
Ga	160.52 ± 3.51	1.25 ± 0.03
Pb	141.86 ± 3.98	2.16 ± 0.09
As	89.14 ± 2.65	41.33 ± 1.29
Ti	56.93 ± 1.95	17.29 ± 0.49
Sb	52.14 ± 1.16	25.66 ± 0.69
Cr	36.93 ± 4.21	29.42 ± 0.16
Sn	33.44 ± 1.21	11.19 ± 1.94
Tl	28.56 ± 0.64	0.03 ± 0.01
Cd	25.28 ± 0.65	0.05 ± 0.00
V	23.94 ± 0.59	9.65 ± 0.17
Ni	18.55 ± 0.83	1.22 ± 0.06
Co	9.92 ± 0.34	1.22 ± 0.03
Be	<LOD	<LOD
Bi	<LOD	<LOD

Data are expressed as mean ± SEM. WE-PM<sub>10</sub>: water-extracted PM<sub>10</sub>; Chel-WE-PM<sub>10</sub>: metals were removed from WE-PM<sub>10</sub> by Chelex 100 resin

EMT and increased capacity of migration and invasion are major mechanisms of tumor progression and metastasis. Although in vitro cell exposure systems cannot fully replicate in vivo conditions, several studies calculated toxicologically relevant doses to assess adverse health effects in human populations. Li et al. outlined in vivo calculations for an individual exposed to PM levels of 79 µg/m<sup>3</sup> over a 24-h period. They estimated dose ranges of particle and particle extracts were 0.2–20 and 0.14–14.1 µg/cm<sup>2</sup>, respectively, which could be used in in vitro toxicology studies and induce in vivo biological effects (Li et al. 2003). Actually, value of 79 µg/m<sup>3</sup> was lower than the mean concentration of PM<sub>10</sub> (117.43 ± 21.51 µg/m<sup>3</sup>) in Beijing during our sampling period, as well as the established limit value (150 µg/m<sup>3</sup>) of PM<sub>10</sub> in Chinese ambient air quality standards (GB3095-2012). We suggested that the concentrations (5–50 µg/ml) chosen in this study were related to real-life PM<sub>10</sub> exposures and the present study provided new evidence for the potential carcinogenicity of WE-PM<sub>10</sub> in lungs.

Metals are main components of PM and have been proposed to make a significant contribution to PM-related adverse health outcomes. Michael et al. compared toxicological effects of different source PM<sub>10</sub> samples on A549 cells and murine macrophages (RAW264.7) and found that the strongest cytotoxic effect was detected in the PM from urban traffic site, which was associated with the highest concentrations of Zn, Cu, Ni and Fe. (Michael et al. 2013). Liu et al. indicated that Pb and Zn factors were strongly associated with ROS generation and inflammatory response in A549 cells exposed to PM<sub>2.5</sub> (collected in Beijing between Mar and May, 2012) (Liu et al. 2014). In vivo study also confirmed that exposure to water-soluble extracts of PM collected from roadside monitoring sites in central London induced transient oxidative stress and inflammation in lung tissues of mice, which was largely attributable to the dissolved metals including Cu, Fe, Mn, V, Ni, and Cr (Pardo et al. 2015). In the present study, we consistently showed that exposure to WE-PM<sub>10</sub> significantly increased the production and secretion of pro-inflammatory cytokine IL6 in A549 cells. Although it remains a challenge to identify the exact component(s) of PM and link them to the observed effects, metals were detected at relatively high levels in this WE-PM<sub>10</sub> sample, such as Zn, Fe, Mn, Cu and As and, moreover, removal of these metals by chelation significantly abrogated the increased IL6 in A549 cells. Therefore, it was reasonable to conclude that cellular inflammatory response to WE-PM<sub>10</sub> was largely attributed to metal components. Sustained inflammation would further lead to lung remodeling, which has been established as a major precursor or “hallmark” for cancer development. Higher levels of systemic and pulmonary IL6 have been commonly observed in lung adenocarcinoma patients, which correlated with poor survival (Gao et al. 2007; Yeh et al. 2006). In this study, STAT3, the major effector of IL6, was activated by tyrosine phosphorylation in WE-PM<sub>10</sub>-exposed A549 cells. Tyrosine-phosphorylated STAT3 has been reported to exist in approximately 50% of lung adenocarcinomas and was correlated positively with IL6 expression in both primary lung adenocarcinomas and cancer-derived cell lines (Gao et al. 2007). Aberrant STAT3 activation triggered by WE-PM<sub>10</sub> in A549 cells could probably increase proliferation, migration, invasion and angiogenesis, and suppress apoptosis. As anticipated, WE-PM<sub>10</sub> further resulted in the enhanced migratory and invasive capacities of cells and also caused an EMT phenotype. Furthermore, nude mice injected with WE-PM<sub>10</sub>-treated A549 cells exhibited increases in both the number and surface area of lung metastatic foci. Removal of metals by Chelex resin significantly suppressed these responses, which was parallel to the changes in inflammation. However, 5–50 µg/ml of WE-PM<sub>10</sub> did not induce proliferative or apoptotic effects in A549 cells (Supplementary material: Fig. S3).

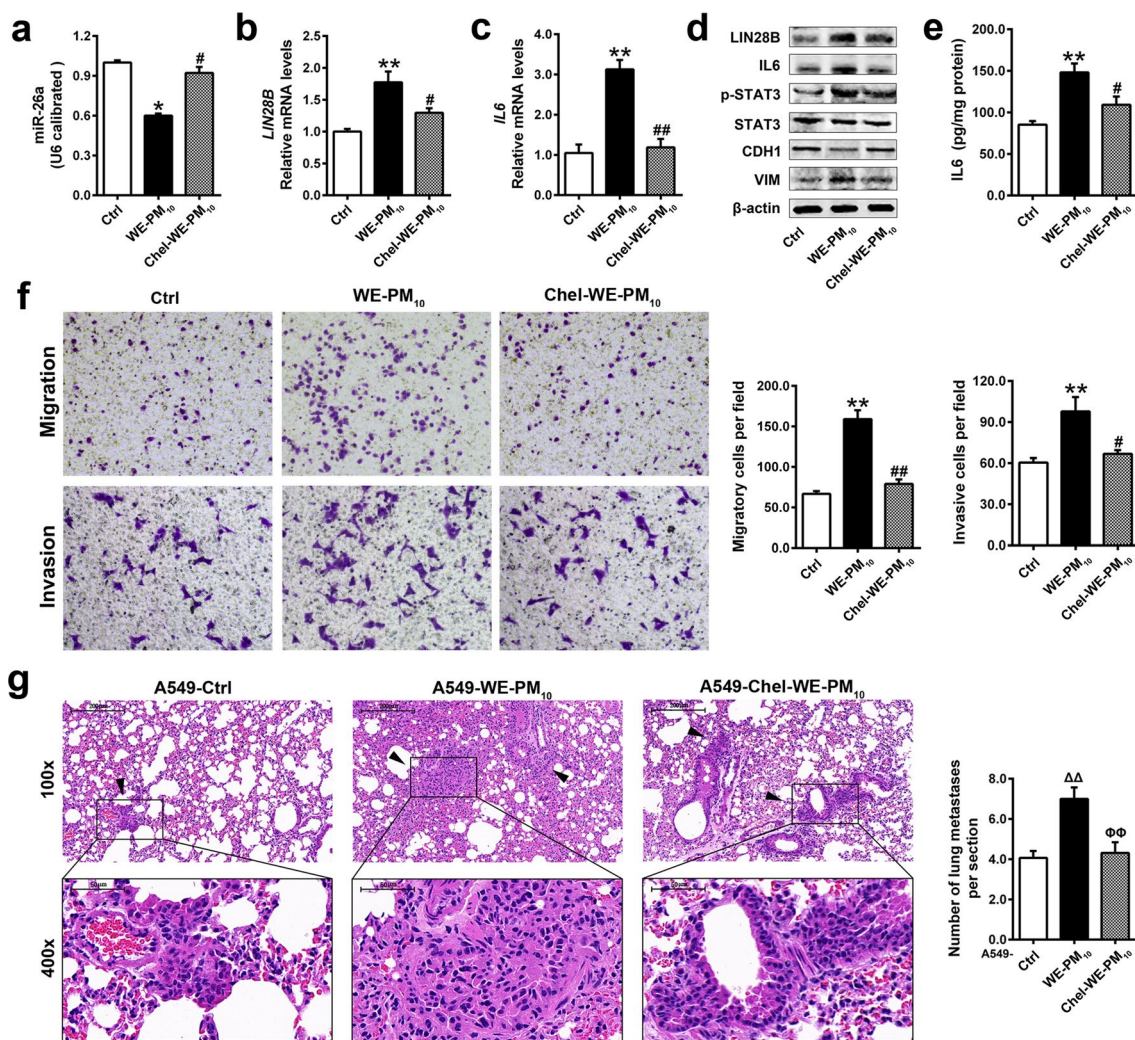


**Fig. 7** Contributions of metals to lung cancer cell inflammation and metastasis. **a** Expression of miR-26a. **b** and **c** mRNA expressions of LIN28B, and IL6. **d** Representative protein bands. **e** Secretion of IL6. **f** Representative photomicrographs ( $\times 100$ ) and average cell number by transwell assays. For **a–f**, A549 cells were treated with 50  $\mu\text{g}/\text{ml}$  WE-PM<sub>10</sub> and Chel-WE-PM<sub>10</sub> for 48 h. **g** Representative images ( $\times 100$  and  $\times 400$ ) and quantification of lung metastases. Arrowheads show microscopic nodules. A549-Ctrl: nude mice were injected with

control A549 cells; A549-PM<sub>10</sub>: nude mice were injected with A549 cells treated with 50  $\mu\text{g}/\text{ml}$  WE-PM<sub>10</sub>; A549-Chel-WE-PM<sub>10</sub>: nude mice were injected with A549 cells treated with Chel-WE-PM<sub>10</sub>. Data were collected from three independent experiments; and for **g**,  $n=5$  mice/group. Data are mean  $\pm$  SEM. \* $p < 0.05$ , \*\* $p < 0.01$  vs. controls; # $p < 0.05$ , ## $p < 0.01$  vs. WE-PM<sub>10</sub>-treated cells;  $\Delta\Delta p < 0.01$  vs. mice in A549-Ctrl group;  $\Phi\Phi p < 0.01$  vs. mice in A549-WE-PM<sub>10</sub> group

Epidemiological studies indicate that exposure to PM causes a global alteration of circulating miRNAs' expression, and miRNAs could be potential biomarkers of some PM-elicited biologic effects or diseases (Bollati et al. 2010; Jardim et al. 2009). In this study, exposure to WE-PM<sub>10</sub> significantly decreased miR-26a in A549 cells, while control and metal-depleted WE-PM<sub>10</sub> did not. MiR-26a functioned as a potential tumor suppressor in multiple cancers, including nasopharyngeal carcinoma (Lu et al. 2011), hepatocellular carcinoma (Yang et al. 2013), lymphoma (Sander et al. 2008), breast cancer (Liu et al. 2015) and esophageal squamous cell carcinoma (Yang et al. 2017). In regard to lung

cancer, the expression of miR-26a was found to be lower in lung cancer specimens than that in the paired normal tissues (Pastuszak-Lewandoska et al. 2016; Zhang et al. 2014). In human lung cancer cells, both miR-26a and miR-26b were also reported to repress proliferation, migration and invasion by targeting cell division cycle 6 (CDC6) (Zhang et al. 2014). Moreover, overexpression of miR-26a decreased proliferation and reversed EMT by targeting enhancer of zeste 2 polycomb repressive complex 2 subunit (EZH2) in docetaxel-resistant lung adenocarcinoma cells (Chen et al. 2017a). However, the role of miR-26a in lung cancer pathogenesis and progression remains controversial

up to now. There are studies which reported that miR-26a enhanced migration and invasion of lung cancer cells through AKT pathway by directly targeting phosphatase and tensin homolog (PTEN) or glycogen synthase kinase 3 beta (GSK3 $\beta$ ) (Lin et al. 2017; Liu et al. 2012), playing a tumor-promoting role. Our current study supported the tumor-suppressing role of miR-26a in lung cancer, because treatment with miR-26a inhibitors promoted migration and invasion of A549 cells, while overexpression of miR-26a by its mimic showed the opposite effects. More importantly, in this study, WE-PM<sub>10</sub>-induced inflammatory and carcinogenic responses were abolished when miR-26a was overexpressed in A549 cells, further suggesting that miR-26a was negatively regulated, at least in part, WE-PM<sub>10</sub>-related lung cancer metastasis.

MiR-26a has been reported to exert either oncogenic or tumor-suppressive functions by regulating a set of target genes in different types of cancers, such as *EZH2* (Chen et al. 2017a; Lu et al. 2011; Sander et al. 2008), *IL6* (Yang et al. 2013), *metadherin (MTDH)* (Yang et al. 2017), *PTEN* (Liu et al. 2012), *GSK3 $\beta$*  (Lin et al. 2017). In this study, treatment with miR-26a inhibitor upregulated LIN28B to promote migration and invasion of A549 cells, while overexpression of miR-26a showed the opposite effects. LIN28B has been known as an emerging oncogenic driver (Viswanathan et al. 2009) that was shown to be dramatically upregulated in non-small cell lung cancer compared to that in paired normal tissues, and the higher levels of LIN28B were found to occur more frequently in stage II/III patients (Wang et al. 2014). In this study, inhibition of LIN28B rescued the upregulation of IL6 and p-STAT3 and offset the enhancement of migration and invasion in A549 cells treated with 50  $\mu$ g/ml of WE-PM<sub>10</sub>, suggesting that WE-PM<sub>10</sub> induced lung cancer cell metastasis via positive regulation of LIN28B. Interestingly, silencing LIN28B in A549 cells also decreased the expression of IL6 and p-STAT3 and, moreover, inhibition of miR-26a failed to increase protein expression of IL6 and p-STAT3 when LIN28B was knocked down, which occurred in parallel to the changes in migration and invasion. These data implied that LIN28B rather than IL6 or STAT3 is the major target gene of miR-26a and that IL6 and STAT3 were major downstream mediators of LIN28B in the lung cancer cell metastatic processes. Notably, it was reported that p-STAT3 had the potential to further inhibit miR-26a (Zhu et al. 2013), which might lead to a vicious cycle finally promoting WE-PM<sub>10</sub>-related metastasis of lung cancer cells.

Mechanistically, miRNAs regulate target genes through binding to their complementary sites in the 3' untranslated region (3' UTR). Through an unbiased *LIN28B*-3' UTR reporter screen, we also found that the 3' UTR of *LIN28B* contained a binding site (AUUACUUGA) that matched miR-26a in humans. Then, we identified that overexpression or inhibition of miR-26a altered the luciferase reporter activity

of wild-type 3' UTR of *LIN28B* but not its mutant 3' UTR in A549 cells. A previous study also indicated that LIN28B was a direct target of miR-26a, and miR-26a overexpression inhibited the endogenous expression of LIN28B in cancer cell lines and xenograft tumors (Fu et al. 2014). In addition, miR-26a could upregulate LIN28B expression in neuroblastoma by targeting its 3' UTR and enhance the expression of let-7d through direct regulation of LIN28B, which might trigger EMT and contribute to the progression of idiopathic pulmonary fibrosis (Beckers et al. 2015; Liang et al. 2016). Our data together with previous studies concluded that the direct regulation of LIN28B expression by miR-26a was a conserved regulatory mode that existed in cancer tissues or cells, further highlighting the importance of this post-transcriptional regulation.

In conclusion, exposure to PM<sub>10</sub>, particularly PM<sub>10</sub>-bound metals, was associated with increased risk of lung cancer progression and metastasis. Furthermore, miR-26a exerted tumor-suppressive functions in the metastatic process of WE-PM<sub>10</sub>-related lung cancer, at least in part, through forming a negative feedback loop with LIN28B–IL6–STAT3.

**Acknowledgements** This work was supported by the National Natural Science Foundation of China [41390240, 21677140 and 21477124]; the Youth Innovation Promotion Association, CAS [217349]; the Knowledge Innovation Program of the Chinese Academy of Sciences [IUEQN201301 and IUEQN201506]; the Natural Science Foundation of Fujian, China [2017J01028].

## Compliance with ethical standards

**Conflict of interest** The authors declare that they have no conflict of interest.

**Ethical approval** All of the animal experiments were carried out in accordance with the guidelines of the Xiamen University Institutional Committee for the Care and Use of Laboratory Animals and the Institutional Animal Ethics Committee of Institute of Urban Environment, Chinese Academy of Sciences. The manuscript did not contain clinical studies or patient data.

## References

- Beckers A, Van Peer G, Carter DR et al (2015) MYCN-driven regulatory mechanisms controlling LIN28B in neuroblastoma. *Cancer Lett* 366(1):123–132. <https://doi.org/10.1016/j.canlet.2015.06.015>
- Bollati V, Marinelli B, Apostoli P et al (2010) Exposure to metal-rich particulate matter modifies the expression of candidate microRNAs in peripheral blood leukocytes. *Environ Health Perspect* 118(6):763–768. <https://doi.org/10.1289/ehp.0901300>
- Chen X, Zhang L, Huang J et al (2016) Long-term exposure to urban air pollution and lung cancer mortality: a 12-year cohort study in Northern China. *Sci Total Environ* 571:855–861. <https://doi.org/10.1016/j.scitotenv.2016.07.064>
- Chen J, Xu Y, Tao L et al (2017a) MiRNA-26a contributes to the acquisition of malignant behaviors of docetaxel-resistant lung

- adenocarcinoma cells through targeting EZH2. *Cell Physiol Biochem* 41(2):583–597. <https://doi.org/10.1159/000457879>
- Chen W, Zheng R, Zhang S et al (2017b) Cancer incidence and mortality in China in 2013: an analysis based on urbanization level. *Chin J Cancer Res* 29(1):1–10. <https://doi.org/10.21147/j.issn.1000-9604.2017.01.01>
- Deng X, Feng N, Zheng M et al (2017) PM2.5 exposure-induced autophagy is mediated by lncRNA loc146880 which also promotes the migration and invasion of lung cancer cells. *BBA-Gen Subj* 1861(2):112–125. <https://doi.org/10.1016/j.bbagen.2016.11.009>
- Fu X, Meng Z, Liang W et al (2014) miR-26a enhances miRNA biogenesis by targeting Lin28B and Zcchc11 to suppress tumor growth and metastasis. *Oncogene* 33(34):4296–4306. <https://doi.org/10.1038/onc.2013.385>
- Gao SP, Mark KG, Leslie K et al (2007) Mutations in the EGFR kinase domain mediate STAT3 activation via IL-6 production in human lung adenocarcinomas. *J Clin Invest* 117(12):3846–3856. <https://doi.org/10.1172/jci31871>
- Guan W, Zheng X, Chung K, Zhong N (2016) Impact of air pollution on the burden of chronic respiratory diseases in China: time for urgent action. *Lancet* 388(10054):1939–1951. [https://doi.org/10.1016/s0140-6736\(16\)31597-5](https://doi.org/10.1016/s0140-6736(16)31597-5)
- Guo Y, Zeng H, Zheng R et al (2016) The association between lung cancer incidence and ambient air pollution in China: a spatiotemporal analysis. *Environ Res* 144(Pt A):60–65. <https://doi.org/10.1016/j.envres.2015.11.004>
- Guo Y, Zeng H, Zheng R et al (2017) The burden of lung cancer mortality attributable to fine particles in China. *Sci Total Environ* 579:1460–1466. <https://doi.org/10.1016/j.scitotenv.2016.11.007>
- Hamra GB, Guha N, Cohen A et al (2014) Outdoor particulate matter exposure and lung cancer: a systematic review and meta-analysis. *Environ Health Perspect* 122(9):906–911. <https://doi.org/10.1289/ehp.1408092>
- IARC (2012) Agents classified by the IARC monographs, volumes 1–109. International Agency for Research on Cancer, Lyon, France
- Jardim MJ, Fry RC, Jaspers I, Dailey L, Diaz-Sanchez D (2009) Disruption of microRNA expression in human airway cells by diesel exhaust particles is linked to tumorigenesis-associated pathways. *Environ Health Perspect* 117(11):1745–1751. <https://doi.org/10.1289/ehp.0900756>
- Li N, Hao M, Phalen RF, Hinds WC, Nel AE (2003) Particulate air pollutants and asthma. A paradigm for the role of oxidative stress in PM-induced adverse health effects. *Clin Immunol* 109(3):250–265. <https://doi.org/10.1016/j.clim.2003.08.006>
- Li X, Lv Y, Gao N et al (2016) microRNA-802/Rnd3 pathway imposes on carcinogenesis and metastasis of fine particulate matter exposure. *Oncotarget* 7(23):35026–35043. <https://doi.org/10.18632/oncotarget.9019>
- Liang H, Liu S, Chen Y et al (2016) miR-26a suppresses EMT by disrupting the Lin28B/let-7d axis: potential cross-talks among miRNAs in IPF. *J Mol Med* 94(6):655–665. <https://doi.org/10.1007/s00109-016-1381-8>
- Lin G, Liu B, Meng Z et al (2017) MiR-26a enhances invasive capacity by suppressing GSK3beta in human lung cancer cells. *Exp Cell Res* 352(2):364–374. <https://doi.org/10.1016/j.yexcr.2017.02.033>
- Liu B, Wu X, Liu B et al (2012) MiR-26a enhances metastasis potential of lung cancer cells via AKT pathway by targeting PTEN. *BBA-Mol Basis Dis* 1822(11):1692–1704. <https://doi.org/10.1016/j.bbadis.2012.07.019>
- Liu Q, Baumgartner J, Zhang Y, Liu Y, Sun Y, Zhang M (2014) Oxidative potential and inflammatory impacts of source apportioned ambient air pollution in Beijing. *Environ Sci Technol* 48(21):12920–12929. <https://doi.org/10.1021/es5029876>
- Liu P, Tang H, Chen B et al (2015) miR-26a suppresses tumour proliferation and metastasis by targeting metadherin in triple negative breast cancer. *Cancer Lett* 357(1):384–392. <https://doi.org/10.1016/j.canlet.2014.11.050>
- Lu J, He M, Wang L et al (2011) MiR-26a inhibits cell growth and tumorigenesis of nasopharyngeal carcinoma through repression of EZH2. *Cancer Res* 71(1):225–233. <https://doi.org/10.1158/0008-5472.can-10-1850>
- Michael S, Montag M, Dott W (2013) Pro-inflammatory effects and oxidative stress in lung macrophages and epithelial cells induced by ambient particulate matter. *Environ Pollut* 183:19–29. <https://doi.org/10.1016/j.envpol.2013.01.026>
- Morales-Barcenas R, Chirino YI, Sanchez-Perez Y et al (2015) Particulate matter (PM10) induces metalloproteinase activity and invasion in airway epithelial cells. *Toxicol Lett* 237(3):167–173. <https://doi.org/10.1016/j.toxlet.2015.06.001>
- Pan H, Wen Z, Huang Y et al (2015) Down-regulation of microRNA-144 in air pollution-related lung cancer. *Sci Rep* 5:14331. <https://doi.org/10.1038/srep14331>
- Pardo M, Shafer MM, Rudich A, Schauer JJ, Rudich Y (2015) Single exposure to near roadway particulate matter leads to confined inflammatory and defense responses: possible role of metals. *Environ Sci Technol* 49(14):8777–8785. <https://doi.org/10.1021/acs.est.5b01449>
- Pastuszek-Lewandoska D, Kordiak J, Czarnecka KH et al (2016) Expression analysis of three miRNAs, miR-26a, miR-29b and miR-519d, in relation to MMP-2 expression level in non-small cell lung cancer patients: a pilot study. *Med Oncol* 33(8):96. <https://doi.org/10.1007/s12032-016-0815-z>
- Raaschou-Nielsen O, Andersen ZJ, Beelen R et al (2013) Air pollution and lung cancer incidence in 17 European cohorts: prospective analyses from the European Study of Cohorts for Air Pollution Effects (ESCAPE). *Lancet Oncol* 14(9):813–822. [https://doi.org/10.1016/s1470-2045\(13\)70279-1](https://doi.org/10.1016/s1470-2045(13)70279-1)
- Raaschou-Nielsen O, Beelen R, Wang M et al (2016) Particulate matter air pollution components and risk for lung cancer. *Environ Int* 87:66–73. <https://doi.org/10.1016/j.envint.2015.11.007>
- Rodriguez-Cotto RI, Ortiz-Martinez MG, Rivera-Ramirez E et al (2014) Particle pollution in Rio de Janeiro, Brazil: increase and decrease of pro-inflammatory cytokines IL-6 and IL-8 in human lung cells. *Environ Pollut* 194:112–120. <https://doi.org/10.1016/j.envpol.2014.07.010>
- Sander S, Bullinger L, Klapproth K et al (2008) MYC stimulates EZH2 expression by repression of its negative regulator miR-26a. *Blood* 112(10):4202–4212. <https://doi.org/10.1182/blood-2008-03-147645>
- Viswanathan SR, Powers JT, Einhorn W et al (2009) Lin28 promotes transformation and is associated with advanced human malignancies. *Nat Genet* 41(7):843–848. <https://doi.org/10.1038/ng.392>
- Wang B, Li K, Jin W et al (2013) Properties and inflammatory effects of various size fractions of ambient particulate matter from Beijing on A549 and J774A.1 cells. *Environ Sci Technol* 47(18):10583–10590. <https://doi.org/10.1021/es401394g>
- Wang L, Zhang L, Wu J et al (2014) IL-1beta-mediated repression of microRNA-101 is crucial for inflammation-promoted lung tumorigenesis. *Cancer Res* 74(17):4720–4730. <https://doi.org/10.1158/0008-5472.can-14-0960>
- Wei J, Li F, Yang J, Liu X, Cho WC (2015) MicroRNAs as regulators of airborne pollution-induced lung inflammation and carcinogenesis. *Arch Toxicol* 89(5):677–685. <https://doi.org/10.1007/s00204-015-1462-4>
- Xu W, Wu Q, Liu X, Tang A, Dore AJ, Heal MR (2016) Characteristics of ammonia, acid gases, and PM2.5 for three typical land-use types in the North China Plain. *Environ Sci Pollut Res Int* 23(2):1158–1172. <https://doi.org/10.1007/s11356-015-5648-3>
- Yang X, Liang L, Zhang X et al (2013) MicroRNA-26a suppresses tumor growth and metastasis of human hepatocellular carcinoma

- by targeting interleukin-6-Stat3 pathway. *Hepatology* 58(1):158–170. <https://doi.org/10.1002/hep.26305>
- Yang C, Zheng S, Liu T et al (2017) Down-regulated miR-26a promotes proliferation, migration, and invasion via negative regulation of MTDH in esophageal squamous cell carcinoma. *FASEB J* 31(5):2114–2122. <https://doi.org/10.1096/fj.201601237>
- Yeh HH, Lai WW, Chen HH, Liu HS, Su WC (2006) Autocrine IL-6-induced Stat3 activation contributes to the pathogenesis of lung adenocarcinoma and malignant pleural effusion. *Oncogene* 25(31):4300–4309. <https://doi.org/10.1038/sj.onc.1209464>
- Zeidler-Erdely PC, Meighan TG, Erdely A et al (2013) Lung tumor promotion by chromium-containing welding particulate matter in a mouse model. *Part Fibre Toxicol* 10:45. <https://doi.org/10.1186/1743-8977-10-45>
- Zhang X, Xiao D, Wang Z et al (2014) MicroRNA-26a/b regulate DNA replication licensing, tumorigenesis, and prognosis by targeting CDC6 in lung cancer. *Mol Cancer Res* 12(11):1535–1546. <https://doi.org/10.1158/1541-7786.mcr-13-0641>
- Zhu H, Vishwamitra D, Curry CV et al (2013) NPM-ALK up-regulates iNOS expression through a STAT3/microRNA-26a-dependent mechanism. *J Pathol* 230(1):82–94. <https://doi.org/10.1002/path.4171>